ELSEVIER

Journal of Hepatology 44 (2006) 383–390

Journal of Hepatology

www.elsevier.com/locate/jhep

Osteopontin expression in normal and fibrotic liver. Altered liver healing in osteopontin-deficient mice

Dionne Lorena[1,2], Ian A. Darby[1,3], Alain-Pierre Gadeau[4], Laetitia Lam Shang Leen[4], Susan Rittling[5], Luís C. Porto[2], Jean Rosenbaum[1], Alexis Desmoulière[1,*]

[1]*Groupe de Recherches pour l'Etude du Foie, Inserm E0362, Institut Fédératif de Recherche 66, Pathologies Infectieuses et Cancers, Université Victor Segalen Bordeaux 2, Bordeaux, France*

[2]*Departamento de Histologia e Embriologia, Universidade do Estado do Rio de Janeiro, Rio de Janeiro, Brazil*

[3]*Wound Healing and Microvascular Biology Group, School of Medical Sciences, RMIT University, Victoria, Australia*

[4]*Inserm U441, Institut Fédératif de Recherche 4, Université Victor Segalen Bordeaux 2, Bordeaux, France*

[5]*Rutgers University, Piscataway, NJ, USA*

***Background/Aims*: Osteopontin has been implicated in numerous physiopathological events. Osteopontin expression in normal and fibrotic liver and liver fibrogenesis in osteopontin-deficient mice were studied.**

***Methods*: Fibrosis was induced in mice and rats by carbon tetrachloride (CCl_4) treatment or bile duct ligation. The liver was used for conventional histology, osteopontin immunohistochemistry and in situ hybridization, or protein and RNA extraction. In mice, necrotic areas and fibrosis were evaluated by quantitative image analysis.**

***Results*: In normal liver, osteopontin mRNA expression was very low. After CCl_4 treatment or bile duct ligation, osteopontin mRNA expression was increased. Osteopontin was expressed by biliary epithelial cells in normal and fibrotic liver. Soon after the beginning of the CCl_4 treatment, osteopontin was also present in inflammatory cells of the necrotic areas. In osteopontin-deficient mice, necrotic areas after a single dose of CCl_4, and fibrosis after chronic CCl_4 treatment were significantly increased as compared with wild-type treated mice.**

***Conclusions*: Our results show that osteopontin expression increases during liver fibrogenesis. Furthermore, osteopontin-deficient mice were more susceptible to CCl_4 treatment, displaying more necrosis during the initial steps (probably due to a deficiency in nitric oxide production) and more fibrosis thereafter. The increase in osteopontin expression observed during liver fibrogenesis may play a protective role.**

***Keywords*: Osteopontin; Liver fibrosis; Carbon tetrachloride; Bile duct ligation; Biliary epithelial cell; Inflammatory cell; Nitric oxide**

1. Introduction

Osteopontin is a phosphorylated acidic glycoprotein which belongs to a family of extracellular matrix proteins, termed 'matricellular' proteins, that function as adaptors and modulators of cell-matrix interactions [1,2]. Matricellular proteins function as both soluble and insoluble proteins. They are capable, as substrates, to support the initial and intermediate stage of cell adhesion, i.e. attachment and spreading; when presented as soluble proteins to cell in a strong adhesive state, they show de-adhesive effects. However, at least in some cases (e.g. in tumours), it has been shown that osteopontin is primarily, if not exclusively, soluble [3].

The study of osteopontin-null mice has revealed roles for osteopontin in a broad range of physiological and pathological processes [4]. Osteopontin expression is increased in response to stress or tissue injury showing an important role particularly in the regulation of inflammation, tissue remodeling, and cell survival [5,6].

Received 30 November 2004; received in revised form 1 July 2005; accepted 9 July 2005; available online 15 August 2005

* Corresponding author. Tel.: +33 557 57 17 71; fax: +33 556 51 40 77.
E-mail address: Alexis.Desmouliere@gref.u-bordeaux2.fr (A. Desmoulière).

0168-8278/$30.00 © 2005 European Association for the Study of the Liver. Published by Elsevier B.V. All rights reserved.
doi:10.1016/j.jhep.2005.07.024

Osteopontin contains an integrin-binding arginine-glycine-aspartate (RGD) sequence. Denhardt et al. [6] suggest that osteopontin can deliver an antiapoptotic extracellular matrix-like signal via multiple ligand-receptor interactions to cells, both adherent and non-adherent.

In adult, osteopontin expression is normally restricted, but upregulation appears during cell injury and pathology. For example, osteopontin mRNA expression was not detected in non-wounded skin, but was upregulated as early as 6 h after injury, mainly at the wound margin; positive cells were essentially inflammatory cells [7]. Osteopontin is known to be expressed by biliary epithelial cells in the normal human liver [8]. Osteopontin expression is increased in the liver during acute inflammation, mostly in macrophages [9,10].

However, little is known about the role of osteopontin during the development of liver fibrosis. Thus, we have studied the expression of osteopontin in normal liver and its modulation during liver fibrogenesis. Furthermore, the role of ospeopontin after hepatic injury was evaluated by using osteopontin-deficient mice [11].

2. Materials and methods

2.1. Experimental animals

Fibrosis was induced in mice and rats by bile duct ligation or CCl_4 treatment (300 μl/kg i.p. for mice, 375 μl/kg by gavage for rats, three times a week). Male mice (wild-type mice, see below, 20–30 g) and Wistar rats (200–250 g) (Charles River, St Aubin-lès-Elbeuf, France) were used. Animals (four animals in each experimental group) were sacrificed at 3, 5 and 7 days after bile duct ligation or at 1–4 days, 2 and 6 weeks after the beginning of CCl_4 treatment. Fibrosis was also induced in male 8–12 weeks of age osteopontin-deficient mice or wild-type littermate by CCl_4 treatment. Wild-type and osteopontin-deficient mice on a (C57BL/6J, 129) mixed background were used [11]. Mice (five animals at least in each experimental group) were sacrificed at 1–4 days after a single dose of CCl_4 or at 1–4 weeks after beginning of the treatment. Serum samples were collected, and the liver was removed. Control animals were used in each case: sham-operated for the bile duct ligation model, and olive oil i.p. (in mice) or per os (in rats) for the CCl_4 model; furthermore, some animals did not undergo any treatment. No differences were observed between all these control groups. All animals were maintained on food and water ad libitum in a conventional animal facility. All experiments were carried out using accepted ethical guidelines.

2.2. Processing of liver tissues

A part of fresh tissue samples was routinely formalin-fixed and paraffin-embedded. Sections (5 μm-thick) were stained with hematoxylin-eosin for routine histology, with Sirius red (Sirius red F3B; BDH Chemicals Ltd, Poole, UK) to allow visualization of fibrosis [12], or processed for immunohistochemistry or in situ hybridization. A part was frozen in liquid nitrogen and used for RNA or protein extraction.

2.3. RNA extraction and northern blot analysis

Total RNA was extracted from liver using the RNeasy Mini kit (Qiagen, Les Ulis, France). A 5 μg amount of total RNA were separated by electrophoresis on a 1% agarose gel containing ethidium bromide. The RNAs were transferred onto a positively charged nylon membrane (Hybond-N+; Amersham, Les Ulis, France) by downward capillary transfer in running buffer. Examination of the stained membrane under UV light was used to confirm the quality of loading and transfer. After ultraviolet cross-linking, prehybridization and hybridization were performed using the ULTRAhyb™ solution (Ambion, Austin, TX) at 42 °C. A rat osteopontin cDNA probe [13] was labelled with [α^{32}P]dCTP by random priming using the Ready-To-Go™ kit (Amersham). To further confirm the loading and transfer accuracy, blots were rehybridized with a rat GAPDH cDNA probe [14]. Signals were acquired and quantified with an Instant Imager (Packard Instrument Company, Meriden, CT, USA) and results were expressed as osteopontin/GAPDH ratios.

2.4. Immunohistochemistry

The following antibodies were used: a goat polyclonal antibody against mouse osteopontin (Sigma, St Louis, Mo, USA), a mouse monoclonal antibody ED1, which labels rat monocytes and macrophages (Serotec, Oxford, UK), and a rat monoclonal antibody recognizing the mouse F4/80 antigen, a glycoprotein expressed by murine macrophages (Abcam, Cambridge, UK). For osteopontin and F4/80 immunohistochemistry, secondary antibodies were rabbit anti-goat or rabbit anti-rat immunoglobulins (DakoCytomation, Trappes, France). After washing, the epitopes were detected with the Envision+−horseradish peroxidase system (DakoCytomation) and revealed with liquid diaminobenzidine as previously described [15]. As negative control, goat, mouse, or rat non-immune immunoglobulin fractions (DakoCytomation) were used. Immunostaining was examined with a Zeiss Axioplan 2 microscope (Carl Zeiss Microscopy, Jena, Germany). Images were acquired with an AxioCam camera (Carl Zeiss Vision, Hallbergmoos, Germany) by means of the AxioVision image processing and analysis system (Carl Zeiss Vision).

2.5. In situ hybridization

The osteopontin probe used was a 1.3 kb sequence cloned into Bluescript M13 vector [13]. Sense and antisense probes for rat osteopontin were prepared by incorporation of digoxigenin-labeled UTP (Roche-Diagnostics, Mannheim, Germany) using linearised plasmid which was then labelled using the appropriate RNA polymerase. Labelled probes were blotted onto nylon filters and efficiency of labelling verified by detection with anti-DIG antibody labelled with alkaline phosphatase (Roche-Diagnostics). Hybridization was carried out in hybridization buffer containing 50% formamide at 37 °C. Post hybridization washes were performed in 50% formamide/2×SSC at 42 °C. Additionally, unbound probe was removed by incubation of sections in RNase A (Sigma). Then, slides were incubated in anti-DIG alkaline phosphatase antibody, and hybrids were detected using NBT/BCIP (Roche-Diagnostics).

2.6. Reverse-transcription polymerase chain reaction (RT-PCR) experiments

RT-PCR was performed essentially as previously described [16]. Total RNA extracted from freshly isolated mouse (Pharmakine, Derio-Bizkaia, Spain) and rat (gift of Dr Theret, INSERM U260, Rennes, France) hepatocytes, and from mouse (gift of Dr Geerts, Laboratory for Liver Cell Biology, Free University Brussels, Belgium) and rat (gift of Dr Paradis, Service d'Anatomie Pathologique, Hôpital Beaujon, Clichy, France) hepatic stellate cells after 2 and 8 days in culture, were used. Hepatocytes and hepatic stellate cells were isolated from Balb/C mice and from Wistar rats. The same samples were used for amplification of the house-keeping gene β-actin. Specific oligonucleotide primers were used: rat osteopontin (forward 5′-CAGTCGATGTCCCTGACGG-3′, reverse 5′-GTTGC TGTCCT GATCAGAGG-3′), mouse osteopontin (forward 5′-TCACTC-CAATCGTCCCTACA-3′, reverse 5′-CTGGA ACATCGTATGGGTA-3′), for β-actin (forward 5′-GTTCC GATGC CCGAGGCTCT-3′, reverse 5′-GCATTTGCG GTGCACGATGGA-3′). The PCR amplification was carried out according to the following program: initial denaturation at 95 °C for 10 min and 30 cycles, each consisting of denaturation at 94 °C for 1 min, annealing at 60 °C for 30 s, and extension at 72 °C for 1 min, followed by a final extension at 72 °C for 7 min in an Eppendorf Mastercycler. The PCR products were resolved on a 2% agarose gel.

2.7. Quantitative image analysis

In wild-type and osteopontin-deficient mice, necrotic areas and fibrosis were evaluated by quantitative image analysis. Images were acquired as above and quantitative data were obtained using a computerized image analysis system (KS 300, Carl Zeiss Vision). The analysis was performed on an average of 25 fields/section using the ×10 objective. Necrosis and fibrosis were expressed as a percentage of necrotic or Sirius red stained areas per field area, respectively. Furthermore, after acute CCl_4 treatment, the number of F4/80 positive cells per field was determined in the centrolobular areas by morphometric analysis using the Image-Pro Plus software package (Media Cybernetics, Carlsbad, Ca, USA). The analysis was performed on an average of 10 fields/section using the ×40 objective. Data were calculated as mean values ± SEM. A Student's *t*-test for unpaired samples was used for statistical analysis. A P value < 0.05 was considered significant.

2.8. Western blotting

Snap frozen liver tissues were glass-homogenized in lysis buffer. As a positive control for inducible nitric oxide synthase (iNOS), peritoneal macrophages of mice treated with lipopolysaccharide (LPS, Sigma) for 24 h were used. Thirty milligrams of proteins were electrophoresed in 7% SDS-polyacrylamide gels and transferred onto Immobilon-P membranes (Millipore, Bedford, MA). Then, membranes were incubated with a rabbit polyclonal antibody against iNOS (Santa Cruz Biotechnology, Santa Cruz, CA), followed by a peroxidase-conjugated goat anti-rabbit antibody (DakoCytomation). Antibody binding was visualized by autoradiography with enhanced chemiluminescence Western blotting reagents (Amersham).

3. Results

3.1. Osteopontin mRNA expression in total mice and rat liver extracts

In normal mice liver, the level of osteopontin mRNA expression was low as shown by Northern blot (Fig. 1). After bile duct ligation, a progressive increase in osteopontin mRNA expression was observed between 3, 5, and 7 days (Fig. 1). After CCl_4 treatment, an important increase in osteopontin mRNA was observed very early at 1–3 days with a decrease at 4 days; then, an increase at 2 and 6 weeks was observed (Fig. 1). In rats, a similar pattern of osteopontin mRNA expression was observed (data not shown).

3.2. Immunohistochemistry and in situ hybridization

By immunohistochemistry, osteopontin was detected in normal liver only in biliary epithelial cells both in mice (Fig. 2(a)) and rats (Fig. 2(d)). After bile duct ligation, proliferating biliary epithelial cells expressed osteopontin (Fig. 2(b) and (e)). In situ hybridization confirmed a high level of osteopontin mRNA expression specifically in proliferating biliary epithelial cells after bile duct ligation in rats (Fig. 2(f)). After CCl_4 treatment, soon after the beginning of the treatment (2 days), osteopontin was observed in necrotic areas around centrolobular veins (Fig. 2(c) and (g)); by in situ hybridization on rat tissue, cells located between necrotic hepatocytes expressed high levels of osteopontin mRNA (Fig. 2(h)). After 2 and 6 weeks of CCl_4 treatment, osteopontin was exclusively present in biliary epithelial cells which proliferated when the development of the lesions (initially in centrolobular areas) involved portal areas (Fig. 2(i)). Soon after the beginning of the CCl_4 treatment (2 days), immunohistochemistry on serial rat tissue sections strongly suggested that cells expressing osteopontin in necrotic areas around centrolobular veins appears to be of monocytes/macrophages origin expressing ED1 (Fig. 3).

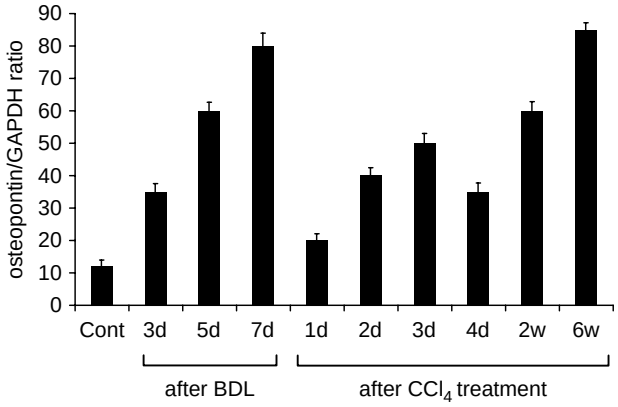

Fig. 1. Osteopontin mRNA expression in total mouse liver extracts. Osteopontin mRNA expression is detectable in normal liver as shown by Northern blot. After bile duct ligation, a progressive increase in osteopontin mRNA expression is observed between 3, 5, and 7 days. After CCl_4 treatment, an important increase in osteopontin mRNA is observed very early with a decrease at 4 days; at 2 and 6 weeks, osteopontin mRNA expression is again increased. The graph shows the mean osteopontin/GAPDH values from three animals per time point. BDL: bile duct ligation.

3.3. Osteopontin RT-PCR analysis in mouse and rat hepatocytes and hepatic stellate cells

In freshly isolated mice hepatocytes (Fig. 4(a) lanes 3, 4, 5), and in mice (Fig. 4(a)) and rat (Fig. 4(c)) hepatic stellate cells cultured for 2 (lane 6) and 8 (lane 7) days, osteopontin transcripts were detected. In freshly isolated rat hepatocytes, osteopontin transcripts were not observed. All PCRs were repeated at least twice with similar results. No signal was observed when the RT reaction was conducted in the absence of the enzyme (Fig. 4, lane 2); all samples expressed β-actin transcripts (Fig. 4(b) and (d)).

3.4. Effect of acute and chronic CCl_4-treatment in osteopontin-deficient and wild-type mice

Aspartate aminotransferase (ASAT) and alanine aminotransferase (ALAT) were increased in wild-type mice, 1–4 days after a single dose of CCl_4 (acute CCl_4 treatment) as compared with non-treated wild-type mice (Table 1). In non-treated mice, values were not different between wild-type and osteopontin-deficient mice. Values were significantly increased in osteopontin-deficient mice 1 day after

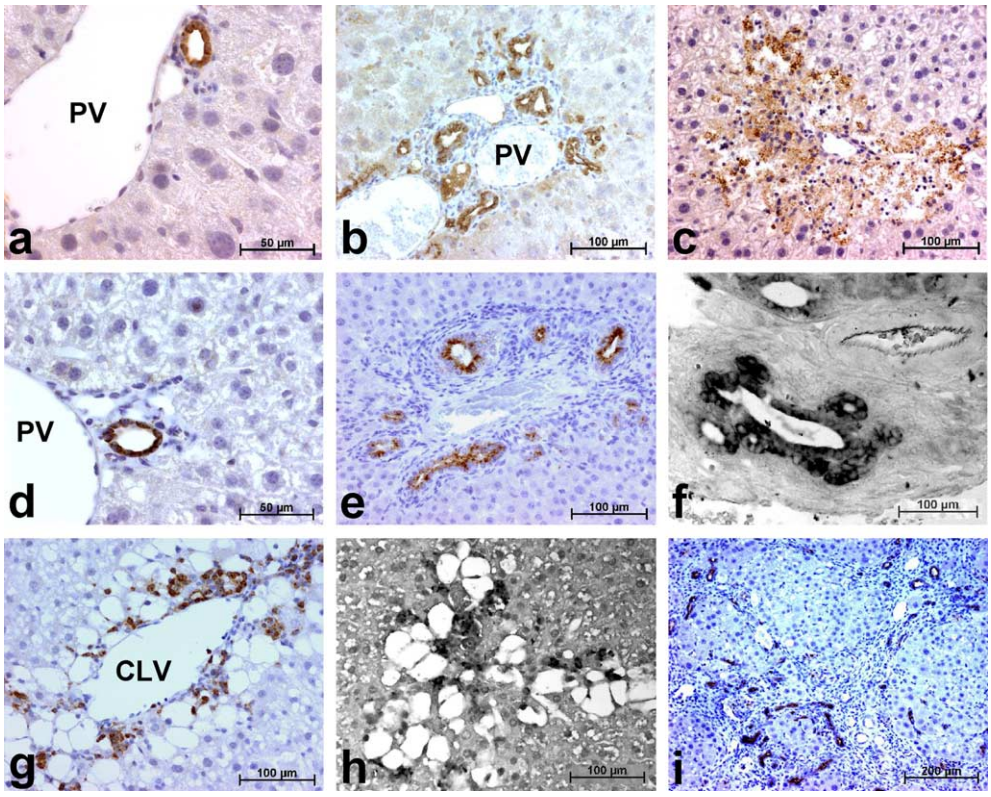

Fig. 2. Immunohistochemistry and in situ hybridization for osteopontin in normal and fibrotic mouse (a–c) and rat (d–i) liver. By immunohistochemistry, osteopontin is detected in normal mouse and rat liver only in biliary epithelial cells (a, d). After bile duct ligation, mouse (b) and rat (e) proliferating biliary epithelial cells express osteopontin; in situ hybridization confirms a high level of osteopontin mRNA expression in rat proliferating biliary epithelial cells (f). Two days after the beginning of the CCl_4 treatment, inflammatory cells in necrotic areas around centrolobular veins express both osteopontin protein (c, g) and mRNA (h). After 6 weeks of CCl_4 treatment in rats, osteopontin is exclusively present in biliary epithelial cells which proliferate when the development of the lesions (initially in centrolobular areas) involves portal areas (i). PV: portal vein; CLV: centrolobular vein.

a single dose of CCl_4, as compared with wild-type mice (Table 1); 2–4 days after a single dose of CCl_4, values did not show statistically significant differences between osteopontin-deficient and wild-type mice (Table 1). As compared to non-treated mice, transaminases were not statistically different in wild-type mice, treated with CCl_4 for 1–4 weeks (chronic CCl_4 treatment; data not shown); at 1–4 weeks after beginning of the treatment, values did not show statistically significant differences between osteopontin-deficient and wild-type mice (data not shown).

After a single dose of CCl_4, necrotic areas were significantly increased in osteopontin-deficient mice at 2 and 3 days as compared with wild-type treated mice (Table 2; Fig. 5). Two and 3 days after a single dose of CCl_4, the number of F4/80 positive cells per field, counted around centrolobular areas, was decreased in osteopontin-deficient

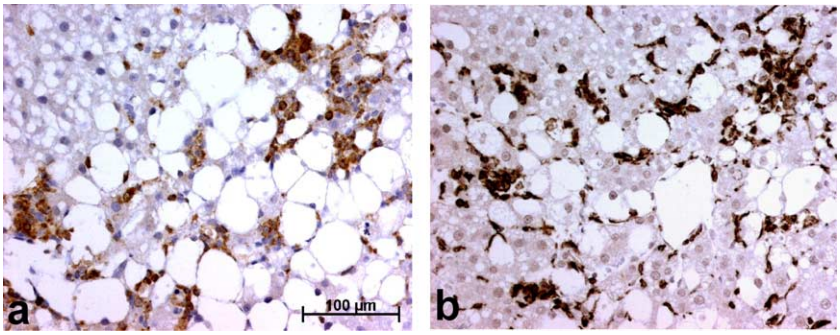

Fig. 3. Immunohistochemistry for osteopontin and ED1 in CCl_4-treated rat liver. Two days after the beginning of the CCl_4 treatment, inflammatory cells in a necrotic area around a centrolobular vein express both osteopontin (a) and ED1 (b), a monocyte/macrophage marker.

mice but the values were not statistically different as compared with wild-type mice (Table 2; Fig. 5). Furthermore, fibrosis was significantly increased at 2 weeks after the beginning of CCl_4 treatment in osteopontin-deficient mice ($1.8 \pm 0.4\%$ of field area) as compared with wild-type mice ($1.4 \pm 0.3\%$, $P < 0.01$) (Fig. 6). At 4 weeks, fibrosis continued to be more prominent in osteopontin-deficient mice ($2.4 \pm 0.5\%$ of field area) as compared with wild-type mice ($2.1 \pm 0.4\%$), but the differences failed to reach statistical significance. Finally, Western blot analysis showed that the expression of iNOS was significantly reduced in osteopontin-deficient mice (52.5 ± 3.4) as compared with wild-type mice (89.1 ± 4.5; $P < 0.02$; Fig. 7).

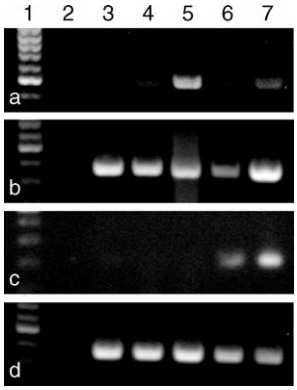

Fig. 4. Expression of osteopontin (a, c) and of β-actin (b, d) transcripts in mouse (a, b) and rat (c, d) hepatocytes (lanes 3, 4, 5) and hepatic stellate cells (lanes 6, 7). The lane 1 contains molecular weight markers; the lane 2 represents a RT reaction where the reverse transcriptase was omitted. Three different isolations of hepatocytes were used (lanes 3, 4, 5). Hepatic stellate cell mRNA extraction were performed after 2 (lane 6) and 8 (lane 7) days in culture. Amplification of β-actin with specific primers confirms the efficiency of the RT reaction. The PCR products were resolved on a 2% agarose gel. The sizes of the predicted products are 491 and 206 bp, respectively, for mouse and rat osteopontin, and 361 bp for β-actin.

4. Discussion

Our results show that osteopontin mRNA expression increases during liver fibrogenesis in both experimental models, bile duct ligation and CCl_4 treatment. Bile duct ligation is a relatively non-inflammatory process and osteopontin expression is seen only in biliary structures. We thus assume that the observed increase in osteopontin mRNA is due to the proliferation of osteopontin-expressing biliary epithelial cells. The role of osteopontin expression in biliary epithelial cells remains to be elucidated. Several studies suggest a role for osteopontin in association with mechanical stress. In cardiomyocytes, the induction of osteopontin is strongly associated with ventricular hypertrophy [17], and osteopontin enhances adaptation of podocytes to mechanical stress [18]. We suggest that osteopontin expressed by biliary epithelial cells may be involved in the management of the stress produced by bile duct ligation and bile stasis. In accordance with our data obtained in the bile duct ligation model, it was shown recently that, in biliary atresia, an up-regulation of osteopontin expression is observed in biliary epithelial cells, which correlates with biliary proliferation and portal fibrosis [19]. In the CCl_4 model, the early and strong increase in osteopontin mRNA expression is due to the numerous osteopontin-expressing inflammatory cells present in the necrotic areas around centrolobular veins. Osteopontin is routinely found at sites of inflammation caused by disease or tissue injury [20]. It has been proposed that, in CCl_4-treated rats, both hepatic stellate cells and activated macrophages express osteopontin [9,21]. It was also shown, in a dietary murine model of non-alcoholic steatohepatitis, an up-regulation of osteopontin predominantly localized in hepatocytes [22]. In the present study, by immunohistochemistry and in situ hybridization, osteopontin was not observed in hepatic stellate cells and hepatocytes. Osteopontin was also not observed in rat hepatic stellate cells by Western blotting soon after isolation, or after 3 and 7 days in culture (data not shown). By RT-PCR on isolated cells, osteopontin transcripts were detected in mice hepatocytes and hepatic stellate cells, and in rat hepatic stellate cells. We can assume that, in our experimentally induced liver fibrosis, osteopontin expressed by hepatic stellate cells or hepatocytes is not or is barely involved in fibrogenesis. Furthermore, osteopontin expression was localised in biliary epithelial cells during biliary atresia [19] and cirrhosis (unpublished data). Furthermore, to our knowledge, in other animal models of fibrosis in kidney [23] or lung [24], or in human diseases [25], osteopontin was never detected in fibrogenic cells which similarly to hepatic stellate cells, acquire a myofibroblastic phenotype when involved in fibrogenesis. A major feature of the inflammatory response is the accumulation of white blood cells at the site of injury, and several studies suggest that osteopontin facilitates the earliest aspects of this process as a regulator of monocyte/macrophage infiltration. For example, osteopontin expressed by tubular epithelium played a pivotal role in mediating peritubular monocyte infiltration consequent to glomerular disease [26], and acute macrophage influx in obstructed kidneys was greatly reduced in osteopontin-deficient mice as compared with wild-type mice [23]. However, the role of osteopontin in macrophage infiltration may depend on the anatomical site and/or the type of inflammatory stimulus: thus, peritoneal instillation of *Mycobacterium bovis* bacillus into osteopontin-deficient mice elicited actually greater cellular exudates as compared with wild-type mice [27], whereas similar numbers of macrophages were observed in wild-type and osteopontin-deficient mice during incisional wound healing [7]. In osteopontin-deficient mice, we have observed that there was a trend towards a lower number of macrophages (F4/80-expressing cells) around centrolobular veins as compared

Table 1
Liver function tests after acute CCl_4 treatment in wild-type and osteopontin-deficient mice

	Aspartate aminotransferase IU.L^{-1}		Alanine aminotransferase IU.L^{-1}	
	Wild-type mice	Osteopontin-deficient mice	Wild-type mice	Osteopontin-deficient mice
Non-treated	85±9	82±12	48±9	55±7
1 day after a single dose of CCl_4	5430±539	10051±1011[a]	11338±1916	22632±1996[b]
2 days after a single dose of CCl_4	1168±105	958±129	3663±1042	2048±319
3 days after a single dose of CCl_4	408±101	554±20	212±24	260±20
4 days after a single dose of CCl_4	288±63	243±57	113±13	94±12

[a] $P<0.02$ as compared with wild-type mice.
[b] $P<0.001$ as compared with wild-type mice.

Table 2
Necrotic areas and number of F4/80 positive cells per field after acute CCl_4 treatment in wild-type and osteopontin-deficient mice

	Necrotic areas (% of field area)		F4/80 positive cells per field	
	Wild-type mice	Osteopontin-deficient mice	Wild-type mice	Osteopontin-deficient mice
Non-treated	/	/	ND	ND
2 days after a single dose of CCl_4	21.6±2.0	25.7±4.5[a]	31.7±6.5	24.5±5.0
3 days after a single dose of CCl_4	11.0±2.6	14.2±2.3[a]	57.9±13.5	37.5±10.3

[a] $P<0.02$ as compared with wild-type mice.

with wild-type treated mice after a single dose of CCl_4. Our data may indicate that osteopontin facilitates macrophage infiltration and accumulation at sites of injury during the initial steps after CCl_4 treatment, underlining the well-known role of osteopontin as a versatile regulator of inflammation [28]. Furthermore, in osteopontin-deficient mice, necrotic areas induced by CCl_4 treatment were significantly increased as compared with treated wild-type mice. Some experiments suggest that osteopontin may interfere with cell death processes, possibly contributing to the survival of cells in response to injury [20]. For example, osteopontin deficient mice exhibit ischemia-induced renal dysfunction which is twice as pronounced as that observed in mice with normal osteopontin expression [29], and, in hydronephrosis induced by ureteral ligation, the kidneys of osteopontin-deficient mice exhibited more interstitial and tubular cell death than did the kidneys of wild-type controls [23]. Together with these studies, our results suggest that osteopontin plays a protective role and enhances hepatocyte survival in CCl_4-treated rats.

Finally, we have observed that osteopontin-deficient mice display more extracellular matrix deposition after chronic CCl_4 treatment. This suggests that, in the CCl_4 model, osteopontin plays either a direct role by reducing fibrosis development, or a protective role by limiting hepatocyte cell death which occurs during the initial inflammatory phase. In several experimental models of renal disease, including ischemia/reperfusion injury [30], ureteral obstruction [23], and cyclosporine A treatment [31], and in heart after aldosterone infusion [32], collagen deposition was reduced in osteopontin-deficient mice. Similarly, during bleomycin-induced lung fibrosis, both type I collagen expression and matrix metalloproteinase-2 were reduced in osteopontin-deficient mice [24]. Therefore, the liver response to damage in osteopontin-deficient mice appears quite distinctive. However, similarly to our data in liver, it has been recently suggested that osteopontin could be a protective mediator of cardiac fibrosis [33]. The mechanism of CCl_4-induced fibrogenesis involves a toxicity of this compound for hepatocytes whereby CCl_4 induces hepatocyte necrosis following its metabolism to a toxic

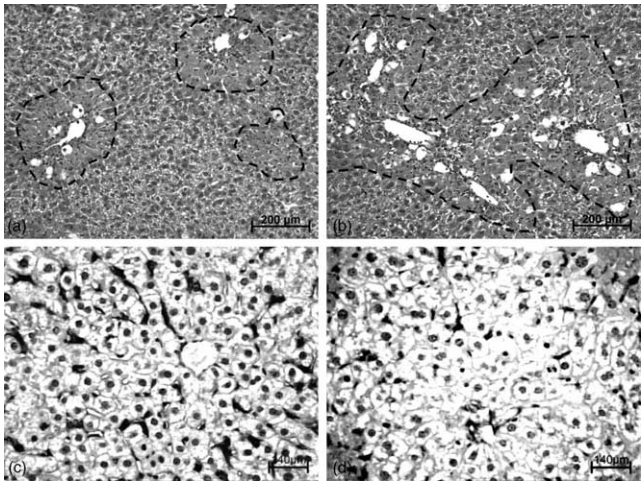

Fig. 5. Hematoxylin-eosin staining (a, b), and immunohistochemistry for F4/80 (c, d) in wild-type (a, c) and osteopontin-deficient (b, d) mice after CCl_4 treatment. Three days after a single dose of CCl_4, necrotic areas (dotted lines) are increased in osteopontin-deficient mice (b) compared with wild-type mice (a). The number of F4/80 positive cells around centrolobular veins is decreased in osteopontin-deficient mice (d) compared with wild-type mice (c).

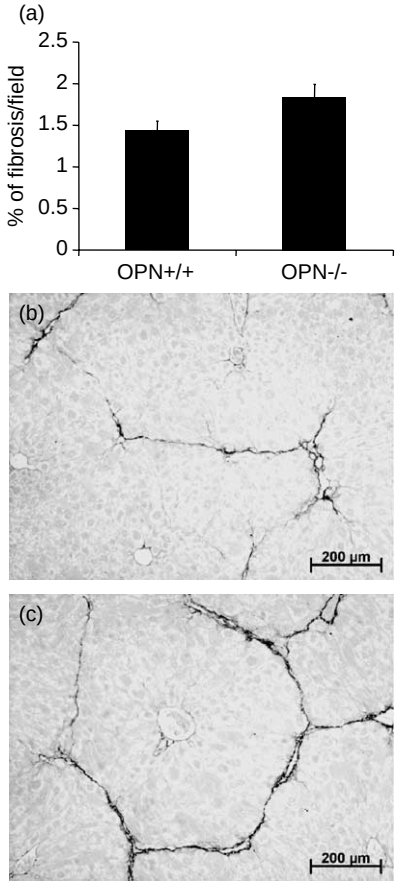

Fig. 6. Liver fibrosis induced by CCl_4 treatment in osteopontin-deficient mice compared with wild-type mice. The quantitative evaluation (a) shows that fibrosis is significantly increased at 2 weeks after the beginning of CCl_4 treatment in osteopontin-deficient mice compared with wild-type mice ($n=12$; $P<0.01$). With Sirius red staining, a slight collagen deposition is observed within centrolobular areas in wild-type mice (b) while delicate septa are present in osteopontin-deficient mice (c).

metabolite [34]. This results in an oxidant stress leading to fibrogenic cell activation and subsequent fibrogenesis. We thus favour the hypothesis that the increased fibrosis seen in osteopontin-deficient mice is secondary to the initial increase in CCl_4 toxicity in those animals. It has been shown that nitric oxide (NO) which is a highly reactive oxidant, produced from L-arginine by parenchymal and non-parenchymal liver cells via the action of iNOS [35,36] plays an hepatoprotective effect: indeed, in mice lacking the gene for iNOS where NO production is decreased, CCl_4-induced hepatotoxicity is exacerbated [37]. Moreover, it has been suggested that osteopontin acts as an autocrine feedback regulator of NO production in macrophages [38], and osteopontin-deficient macrophages produce less NO [39]. We have seen that, after acute CCl_4 treatment, liver iNOS expression is decreased in osteopontin-deficient mice as compared with wild-type mice; we suggest that the decreased expression of iNOS leading to a deficiency in NO production, is responsible at least in part for the increase of CCl_4 toxicity observed in osteopontin-deficient mice.

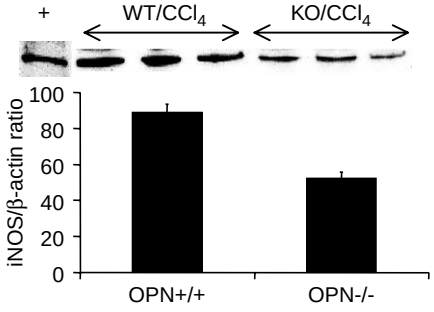

Fig. 7. iNOS expression in CCl_4-treated osteopontin-deficient mice compared with CCl_4-treated wild-type mice. As a positive control for iNOS (+), peritoneal macrophages of mice treated with lipopolysaccharide for 1 day were used. The upper part of the figure shows representative Western blotting for three wild-type mice and three osteopontin-deficient mice. Equivalent loading was confirmed by Ponceau staining of the blot. To further confirm the loading, blots were rehybridized with a mouse monoclonal antibody against β-actin. The signals were detected at 130 kDa for iNOS and 45 kDa for β-actin. The signals were quantified (arbitrary units) with the Kodack 1D Image Analysis Software (Eastman Kodak Company, Rochester, NY). Data were calculated as mean values ± SEM. A Student's *t*-test for unpaired samples was used for statistical analysis. A P value <0.05 was considered significant. The graph shows the mean iNOS/β-actin values from five animals per time point. iNOS expression is significantly reduced in osteopontin-deficient mice compared with wild-type mice ($P<0.02$).

In conclusion, our results show that osteopontin mRNA expression increases during liver fibrogenesis in both the CCl_4 model, through synthesis by inflammatory cells, and the bile duct ligation model, where osteopontin-expressing biliary epithelial cells proliferate. Furthermore, osteopontin-deficient mice were more susceptible to CCl_4 treatment, displaying more necrosis during the initial steps (probably due to a deficiency in NO production) and more extracellular matrix deposition thereafter, suggesting that osteopontin is able to reduce the severity of the lesion developing during hepatic fibrosis.

Acknowledgements

We thank the staff of the Biochemistry Department of Pellegrin Hospital (Bordeaux, France) for performing liver function tests, Dr Paradis (Service d'Anatomie Pathologique, Hôpital Beaujon, Clichy, France) for rat hepatic stellate cell protein and mRNA extracts, Dr Geerts (Laboratory for Liver Cell Biology, Free University Brussels, Belgium) for mouse hepatic stellate cell mRNA extracts, and Dr Theret (INSERM U260, Rennes, France) for rat hepatocyte mRNA extracts. We are very grateful to Chantal Combe (INSERM E0362, Bordeaux, France) for technical help. This work was supported in part by the Région Aquitaine, and a visiting fellowship awarded to Ian A. Darby by the University of Bordeaux 2. Dionne Lorena was recipient of a fellowship from CAPES (Brazil).

References

[1] Murphy-Ullrich JE. The de-adhesive activity of matricellular proteins: is intermediate cell adhesion an adaptive state? J Clin Invest 2001; 107:785–790.

[2] Sage EH. Regulation of interactions between cells and extracellular matrix: a command performance on several stages. J Clin Invest 2001; 107:781–783.

[3] Rittling SR, Chen Y, Feng F, Wu Y. Tumor-derived osteopontin is soluble, not matrix associated. J Biol Chem 2002;277:9175–9182.

[4] Rittling SR, Denhardt DT. Osteopontin function in pathology: lessons from osteopontin-deficient mice. Exp Nephrol 1999;7:103–113.

[5] O'Regan A, Berman JS. Osteopontin: a key cytokine in cell-mediated and granulomatous inflammation. Int J Exp Pathol 2000;81:373–390.

[6] Denhardt DT, Noda M, O'Regan AW, Pavlin D, Berman JS. Osteopontin as a means to cope with environmental insults: regulation of inflammation, tissue remodeling, and cell survival. J Clin Invest 2001;107:1055–1061.

[7] Liaw L, Birk DE, Ballas CB, Whitsitt JS, Davidson JM, Hogan BL. Altered wound healing in mice lacking a functional osteopontin gene (spp1). J Clin Invest 1998;101:1468–1478.

[8] Brown LF, Berse B, Van de Water L, Papadopoulos-Sergiou A, Perruzzi CA, Manseau EJ, et al. Expression and distribution of osteopontin in human tissues: widespread association with luminal epithelial surfaces. Mol Biol Cell 1992;3:1169–1180.

[9] Kawashima R, Mochida S, Matsui A, YouLuTuZ Y, Ishikawa K, Toshima K, et al. Expression of osteopontin in Kupffer cells and hepatic macrophages and stellate cells in rat liver after carbon tetrachloride intoxication: a possible factor for macrophage migration into hepatic necrotic areas. Biochem Biophys Res Commun 1999;256: 527–531.

[10] Wang Y, Mochida S, Kawashima R, Inao M, Matsui A, YouLuTuZ Y, et al. Increased expression of osteopontin in activated Kupffer cells and hepatic macrophages during macrophage migration in Propionibacterium acnes-treated rat liver. J Gastroenterol 2000;35:696–701.

[11] Rittling SR, Matsumoto HN, McKee MD, Nanci A, An XR, Novick KE, et al. Mice lacking osteopontin show normal development and bone structure but display altered osteoclast formation in vitro. J Bone Miner Res 1998;13:1101–1111.

[12] Waldrop FS, Puchtler H. Light microscopic distinction of collagens in hepatic cirrhosis. Histochemistry 1982;74:487–491.

[13] Gadeau AP, Campan M, Millet D, Candresse T, Desgranges C. Osteopontin overexpression is associated with arterial smooth muscle cell proliferation in vitro. Arterioscler Thromb 1993;13:120–125.

[14] Fort P, Marty L, Piechaczyk M, el Sabrouty S, Dani C, Jeanteur P, et al. Various rat adult tissues express only one major mRNA species from the glyceraldehyde-3-phosphate-dehydrogenase multigenic family. Nucleic Acids Res 1985;13:1431–1442.

[15] Uchio K, Tuchweber B, Manabe N, Gabbiani G, Rosenbaum J, Desmoulière A. Cellular retinol-binding protein-1 expression and modulation during in vivo and in vitro myofibroblastic differentiation of rat hepatic stellate cells and portal fibroblasts. Lab Invest 2002;82: 619–628.

[16] Pillois X, Chaulet H, Belloc I, Dupuch F, Desgranges C, Gadeau AP. Nucleotide receptors involved in UTP-induced rat arterial smooth muscle cell migration. Circ Res 2002;90:678–681.

[17] Graf K, Do YS, Ashizawa N, Meehan WP, Giachelli CM, Marboe CC, et al. Myocardial osteopontin expression is associated with left ventricular hypertrophy. Circulation 1997;96:3063–3071.

[18] Endlich N, Sunohara M, Nietfeld W, Wolski EW, Schiwek D, Kranzlin B, et al. Analysis of differential gene expression in stretched podocytes: osteopontin enhances adaptation of podocytes to mechanical stress. FASEB J 2002;16:1850–1852.

[19] Whitington PF, Malladi P, Melin-Aldana H, Azzam R, Mack CL, Sahai A. Expression of osteopontin correlates with portal biliary proliferation and fibrosis in biliary atresia. Pediatr Res 2005;837–844.

[20] Denhardt DT, Giachelli CM, Rittling SR. Role of osteopontin in cellular signaling and toxicant injury. Annu Rev Pharmacol Toxicol 2001;41:723–749.

[21] Lee SH, Seo GS, Park YN, Yoo TM, Sohn DH. Effects and regulation of osteopontin in rat hepatic stellate cells. Biochem Pharmacol 2004; 68:2367–2378.

[22] Sahai A, Malladi P, Melin-Aldana H, Green RM, Whitington PF. Upregulation of osteopontin is involved in the development of nonalcoholic steatohepatitis in a diatery murine model. Am J Physiol Gastrointest Liver Physiol 2004;287:G264–G273.

[23] Ophascharoensuk V, Giachelli CM, Gordon K, Hughes J, Pichler R, Brown P, et al. Obstructive uropathy in the mouse: role of osteopontin in interstitial fibrosis and apoptosis. Kidney Int 1999;56:571–580.

[24] Berman JS, Serlin D, Li X, Whitley G, Hayes J, Rishikof DC, et al. Altered bleomycin-induced lung fibrosis in osteopontin-deficient mice. Am J Physiol Lung Cell Mol Physiol 2004;286:L1311–L1318.

[25] Junaid A, Amara FM. Osteopontin: correlation with interstitial fibrosis in human diabetic kidney and PI3-kinase-mediated enhancement of expression by glucose in human proximal tubular epithelial cells. Histopathology 2004;44:136–146.

[26] Okada H, Moriwaki K, Kalluri R, Takenaka T, Imai H, Ban S, et al. Osteopontin expressed by renal tubular epithelium mediates interstitial monocyte infiltration in rats. Am J Physiol Renal Physiol 2000; 278:F110–F121.

[27] Nau GJ, Guilfoile P, Chupp GL, Berman JS, Kim SJ, Kornfeld H, et al. A chemoattractant cytokine associated with granulomas in tuberculosis and silicosis. Proc Natl Acad Sci USA 1997;94:6414–6419.

[28] Giachelli CM, Steitz S. Osteopontin: a versatile regulator of inflammation and biomineralization. Matrix Biol 2000;19:615–622.

[29] Noiri E, Dickman K, Miller F, Romanov G, Romanov VI, Shaw R, et al. Reduced tolerance to acute renal ischemia in mice with a targeted disruption of the osteopontin gene. Kidney Int 1999;56: 74–82.

[30] Persy VP, Verhulst A, Ysebaert DK, De Greef KE, De Broe ME. Reduced postischemic macrophage infiltration and interstitial fibrosis in osteopontin knockout mice. Kidney Int 2003;63:543–553.

[31] Mazzali M, Hughes J, Dantas M, Liaw L, Steitz S, Alpers CE, et al. Effects of cyclosporine in osteopontin null mice. Kidney Int 2002;62: 78–85.

[32] Sam F, Xie Z, Ooi H, Kerstetter DL, Colucci WS, Singh M, et al. Mice lacking osteopontin exhibit increased left ventricular dilation and reduced fibrosis after aldosterone infusion. Am J Hypertens 2004;17: 188–193.

[33] Graf K, Stawowy P. Osteopontin: a protective mediator of cardiac fibrosis? Hypertension 2004;44:809–810.

[34] Recknagel RO, Glende Jr EA, Dolak JA, Waller RL. Mechanisms of carbon tetrachloride toxicity. Pharmacol Ther 1989;43:139–154.

[35] Geller DA, Lowenstein CJ, Shapiro RA, Nussler AK, Di Silvio M, Wang SC, et al. Molecular cloning and expression of inducible nitric oxide synthase from human hepatocytes. Proc Natl Acad Sci USA 1993;90:3491–3495.

[36] Laskin DL, Heck DE, Gardner CR, Feder LS, Laskin JD. Distincts patterns of nitric oxide production in hepatic macrophages and endothelial cells following acute endotoxemia. J Leucocyte Biol 1994;56:751–758.

[37] Morio LA, Chiu H, Sprowles KA, Zhou P, Heck DE, Gordon MK, et al. Distinct roles of tumor necrosis factor-alpha and nitric oxide in acute liver injury induced by carbon tetrachloride in mice. Toxicol Appl Pharmacol 2001;172:44–51.

[38] Guo H, Cai CQ, Schroeder RA, Kuo PC. Osteopontin is a negative feedback regulator of nitric oxide synthesis in murine macrophages. J Immunol 2001;166:1079–1086.

[39] Bourassa B, Monaghan S, Rittling SR. Impaired anti-tumor cytotoxicity of macrophages from osteopontin-deficient mice. Cell Immunol 2004;227:1–11.